SUPPLEMENTAL MATERIAL

Haluszczak et al., http://www.jem.org/cgi/content/full/jem.20081829/DC1

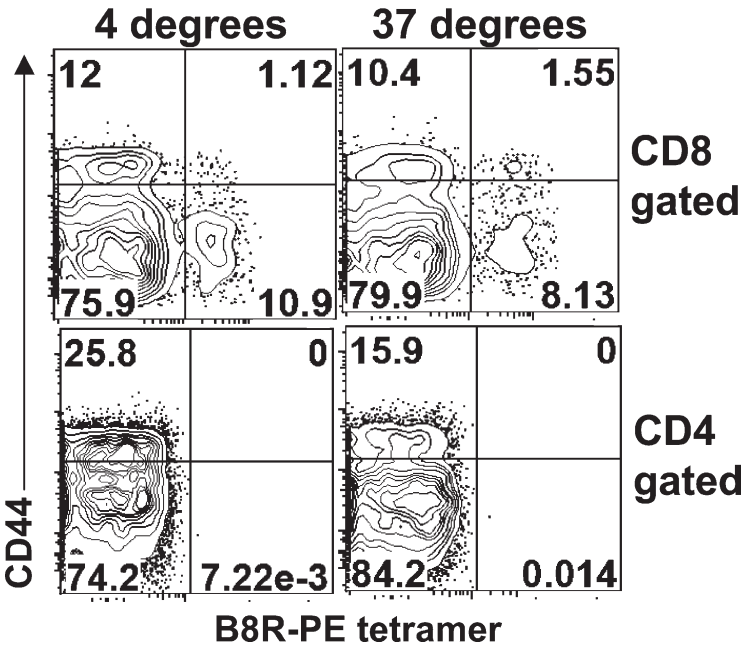

Figure S1. Minimal impact of tetramer staining conditions on recovery of tetramer binding CD44^{hi} cells from unprimed mice. Spleen and LN cells were isolated from unimmunized B6 mice and subjected to tetramer enrichment. In these experiments, tetramer binding was performed at either 4 or 37°C, as indicated, in the absence of anti-CD8 antibody. Cells were enriched using anti–PE-coupled magnetic particles, and the data shown are gated on CD3-positive events that were negative for the dump cocktail (CD11b, CD11c, F4/80, and B220). In this case, CD4 and CD8 were stained individually (as indicated) on the column-bound pool. Similar data were observed in a separate experiment.

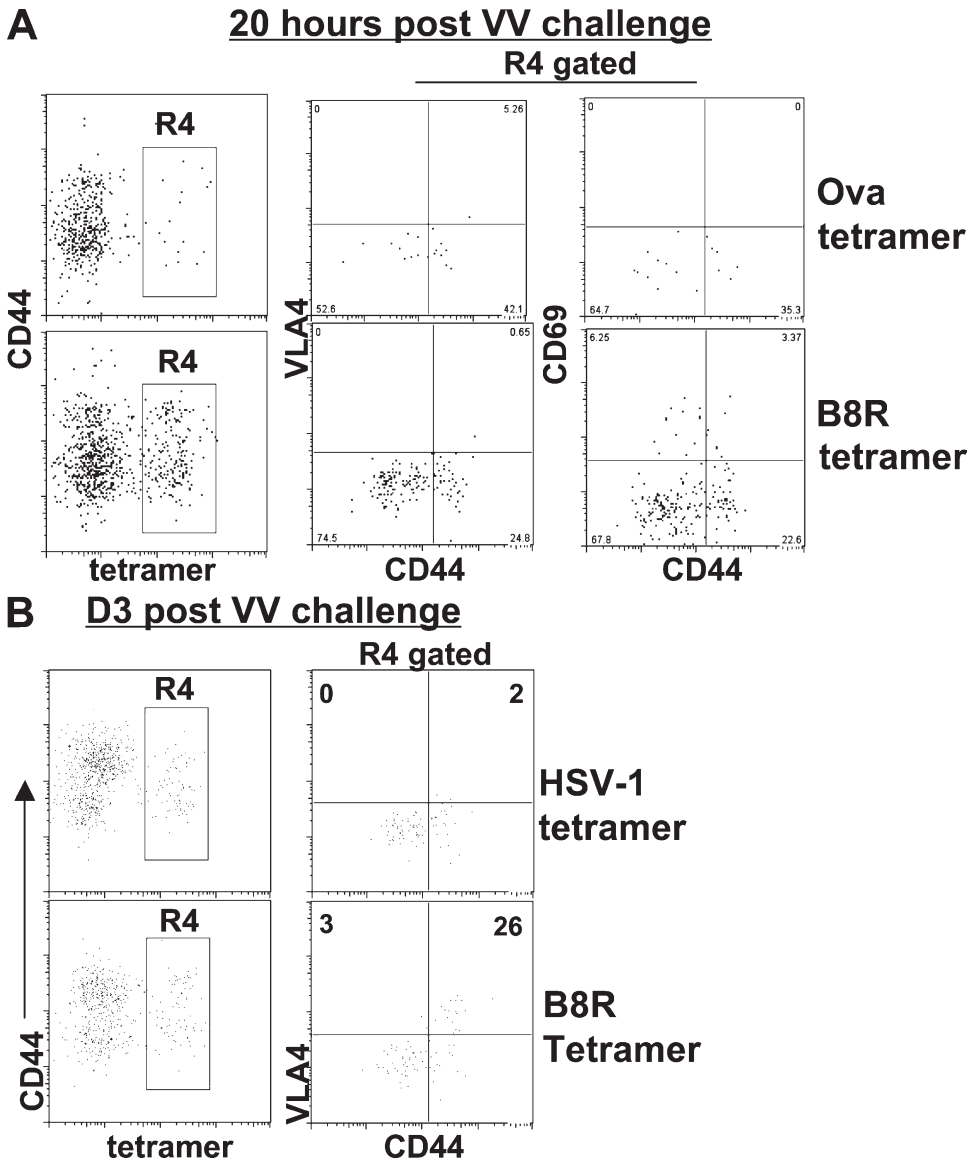

Figure S2. T cells identified by tetramer staining and magnetic bead isolation are antigen specific. B6 mice were challenged with VV-WR and, at the indicated time points, HSV-, Ova,- or B8R-specific T cells were isolated by tetramer staining and magnetic bead separation as described in Fig. 1. Far left dot plots in A and B show gating on all tetramer+ events and the right dot plots indicate the phenotype of either HSV or B8R tetramer + events with respect to the indicated markers. Only cells with the B8R tetramer from VV-challenged mice show signs of phenotypic activation. These data are representative of 3 independent experiments.

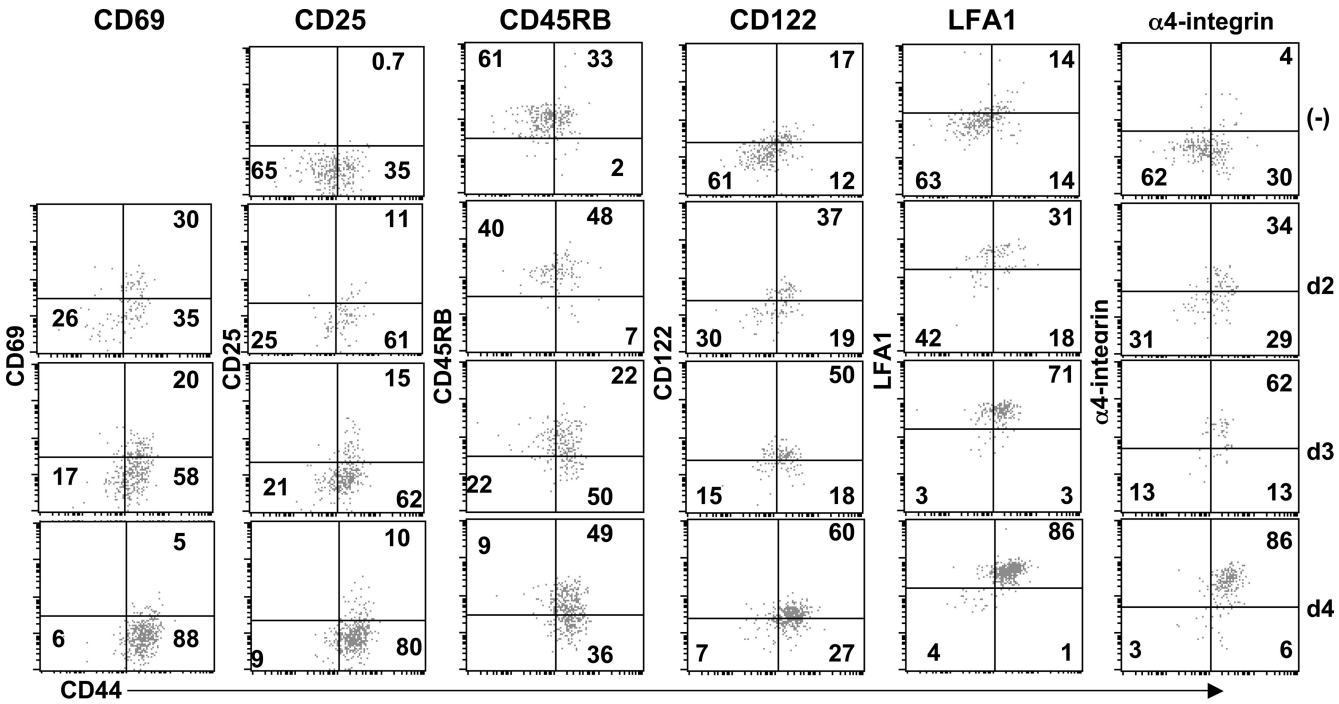

Figure S3. Peptide immunization results in an activation phenotype of B8R-specific T cells similar to that observed following VV-WR challenge. B7 mice were immunized i.v. with 100 µg B8R peptide in combination with 50 µg of the anti-CD40 antibody FGK45. On the indicated time points, B8R-specific T cells were isolated from the spleens, as described in Fig. 1, and analyzed for their expression of the indicated activation markers. Data shown was gated on all $CD8^+B220^-CD3^+$ events. Data is representative of three to four mice per time point from two independent experiments.

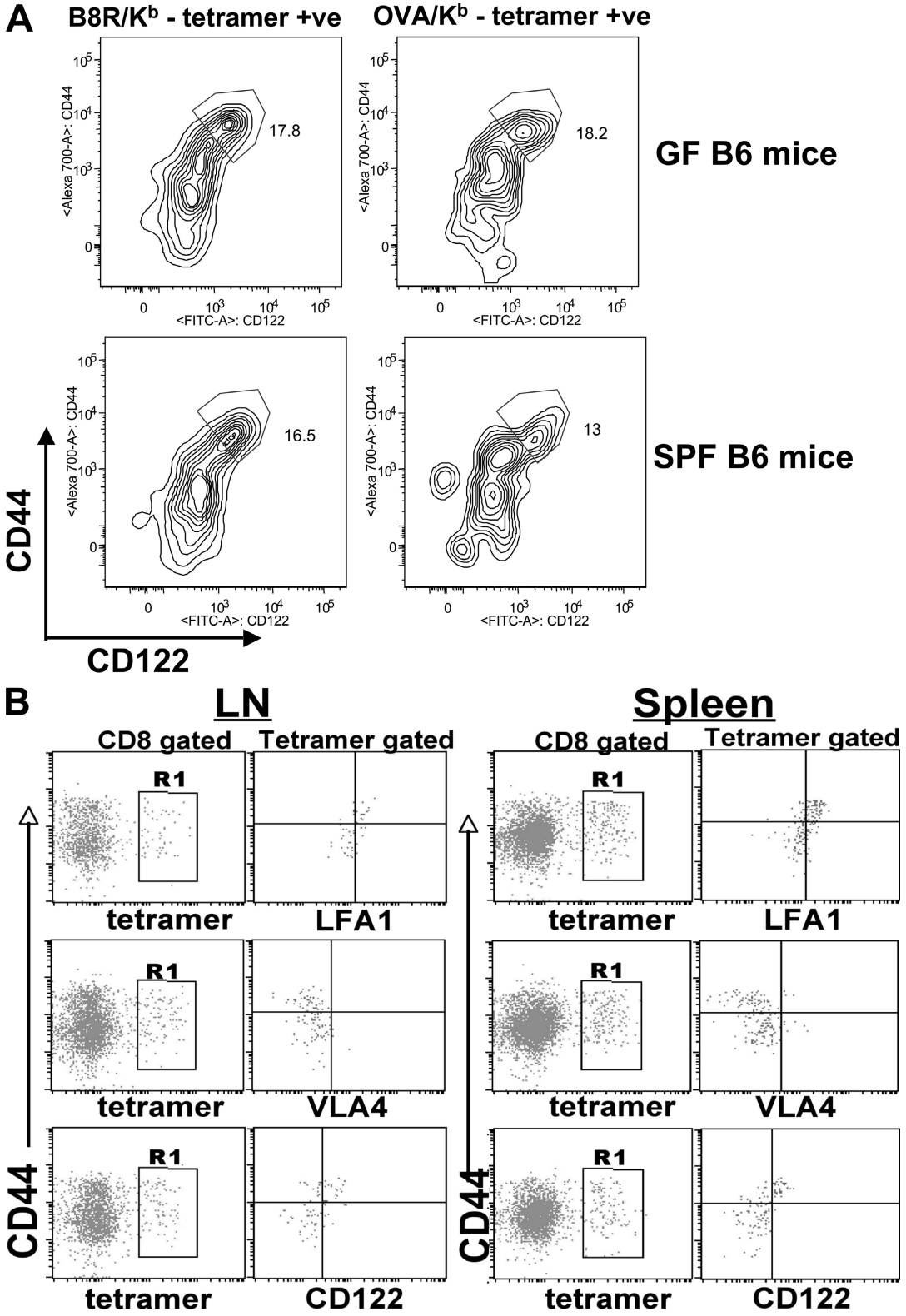

Figure S4. Phenotype of CD44^{hi} tetramer^{+} T cells from unprimed animals isolated from spleen and LN. (A) Spleen and LN cells were isolated from SPF or GF mice and isolated for binding to B8R/K^{b} or OVA/K^{b} tetramer as in Fig. 4. Cells were gated on dump-ve, CD3^{+}CD8^{+}tetramer+ve cells (for the tetramer indicated) and staining for CD44 and CD122 is shown. (B) LN and spleen cells were isolated, stained with B8R tetramer, and isolated by magnetic column separation as described in the Materials and methods and Fig. 5. The phenotype of all CD8^{+}B220^{-}CD3^{+}tetramer^{+} events are shown with respect to the indicated markers. (VLA-4 indicates staining for α4-integrin). These data are representative of five independent experiments.

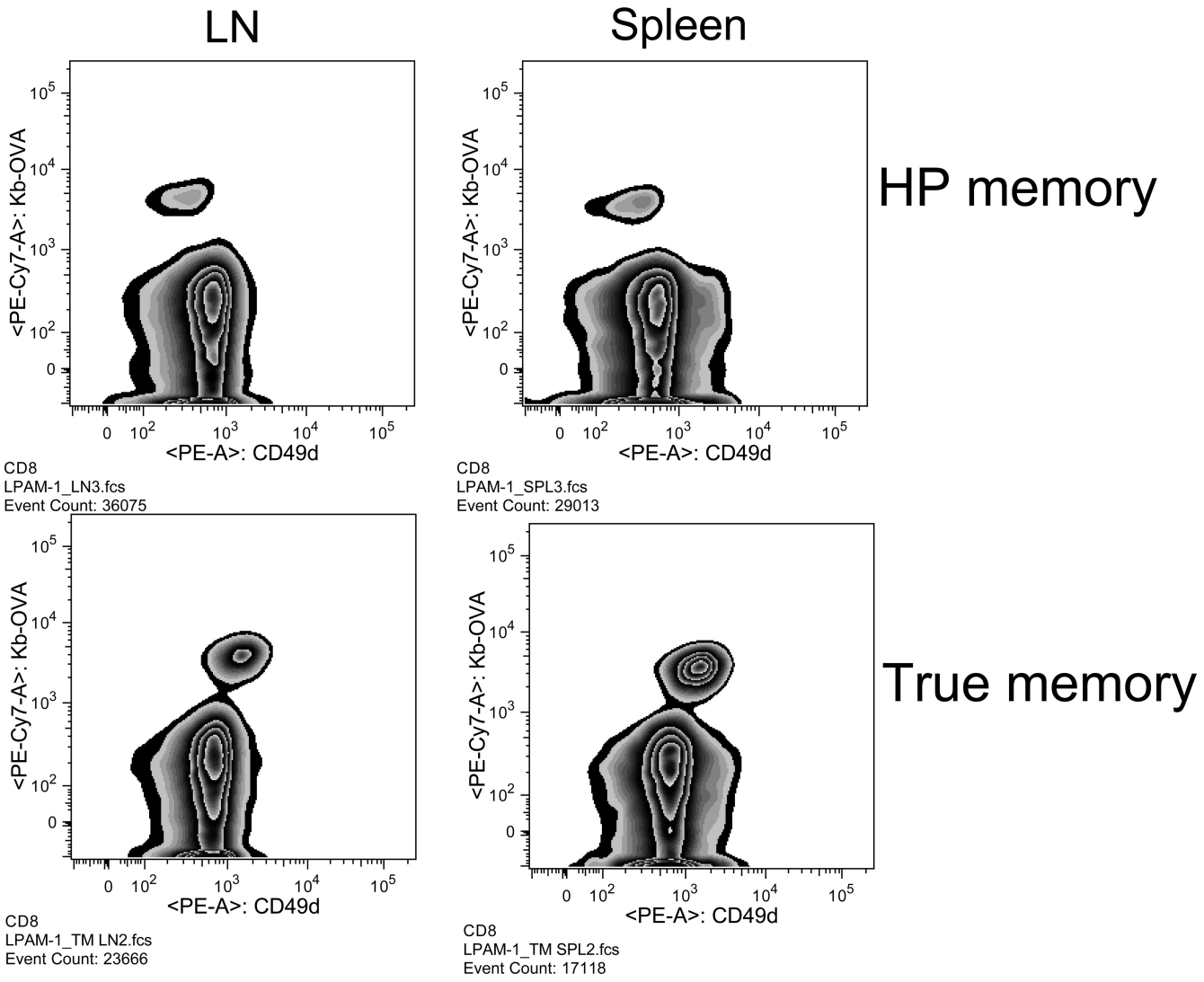

Figure S5. Expression of α4-integrin by antigen-driven versus HP memory OT-I T cells. HP and antigen-driven (true memory) OT-I CD8 T cells were generated after adoptive transfer of naive OT-I cells, as described for Fig. 5 B and the Materials and methods. At least 30 d after OT-I adoptive transfer, spleen and LN cells were isolated and stained for flow cytometry. Data are gated on total CD8 T cells, with donor OT-I cells identified using Ova/K^b tetramer. Staining for α4-integrin is indicated. These data are representative of at least three experiments, with two to three mice per group.